Prediction accuracy analysis from orbital elements generated for a new space object catalogue

James Bennett, Michael Lachut, Ben Greene
SERC Limited, Mt Stromlo Observatory, Cotter Road, Weston Creek, ACT, 2611, Australia
Steve Gehly
SPACE Research Centre, RMIT University, 124 La Trobe Street, Melbourne VIC 3000, Australia
David Kooymans, James Allworth, Alex Pollard, Craig Smith
EOS Space Systems Pty Ltd, Mt Stromlo Observatory, Cotter Road, Weston Creek ACT 2611, Australia

ABSTRACT

The Space Environment Research Centre (SERC) is building a space object catalogue to provide accurate and reliable orbital information for a number of applications. Orbital elements are generated by fitting optical and laser tracking data from tracking assets located in Australia.

This paper reports on the orbital prediction accuracy achieved. The data processing and fusion methodologies are described that improve accuracy and ensure the orbit determination process is not corrupted by erroneous data. Additional information from the data is also obtained by estimating the rates of change of the observation arcs. When the angles and range observation data are fused, the accurate 6-dimensional data is used to generate state vectors directly from the observations. The orbit prediction improvements form a critical component of a Conjunction Assessment capability that is being developed and the progress of the automatic generation of orbit elements is reported here.

1. INTRODUCTION

SERC is a collaboration between EOS Space Systems Pty Ltd, Australia (EOS), RMIT University, Australia (RMIT), The Australian National University, Australia (ANU), Optus Satellite Systems, Australia (Optus), Lockheed Martin Australia (LMC), and the National Institute for Information and Communications Technology, Japan (NICT). The goal is to demonstrate the perturbation of an on-orbit object using photon pressure delivered from ground-based lasers. If the laser manoeuvre is successful and sufficient for conjunction avoidance, then a potential mitigation strategy exists to slow the growth of the debris field in low-Earth orbit.

The decision to engage a debris object to perturb its orbit must be performed with an accurate forecast of the future collision risk. The prediction of whether the laser manoeuvre intervention will reduce or increase the collision risk is important for an operational conjunction assessments system. These assessments must include the objects of interest in the original conjunction alert as well as all objects in the vicinity.

As well as the low-Earth orbit debris laser manoeuvre mission, the Space Asset Management (SAM) group at SERC is building a conjunction assessment software suite which will assist satellite operators to make informed decisions on whether to manoeuvre their assets. To facilitate this service, SERC is building a Space Object Catalogue (SOC) using observations collected by partner tracking assets in Australia. SAM is working closely with Optus to build a conjunction and threat warning capability. Research and development in SAM is focused in the following areas:

1. Precision tracking and effective data fusion;
2. Parallelized conjunction assessments on a GPU (can also run parallelized on a CPU);
3. Nonlinear, non-Gaussian error propagation and actionable collision risk information generation;
4. Accurate orbit determinations and propagations;
5. Object characterizations and associations, spin and orientation determination, force modelling;
6. Automated and optimal sensor scheduling.

This paper reports on the recent tracking efforts for a subset of objects identified in close approaches with Optus satellites and the progress towards an automated orbital element generation service for the catalogue is also discussed.

2. TRACKING FACILITIES

Data from two tracking facilities was used in this study. The first site is EOS Space Systems' Space Debris Tracking Station, located on Mt Stromlo, ACT. The other site is located at Learmonth, WA and is a joint project between EOS and Lockheed Martin with support from the Australian Government. The location of the sites is depicted in Fig. 1 and both sites are capable of passive optical tracking and active laser ranging. The majority of the data collected for this study was passive optical observations from Mt Stromlo. The laser ranging measurements used in the post-processing analysis below were collected from Learmonth.

Fig. 1. Map showing the locations of the tracking facilities. Mt Stromlo is on the right, Learmonth is on the left.

3. DATA COLLECTION

A data collection campaign started on May 22nd 2017 and is ongoing. Several objectives were designed to be met with the data collection campaign:

1. Test the optimal scheduling algorithms;
2. Automate the data post-processing and orbit element generation;
3. Collect data to facilitate the improvement of the conjunction assessments and nonlinear/non-Gaussian error propagation studies;
4. Generate light curves using the automated light curve generation software for object orientation and spin determination;
5. Characterize and maintain custody of the objects that come in close proximity to Optus satellite assets.

Due to incomplete knowledge of the characteristics of orbiting objects and the perturbing forces acting upon them, regular observations are required to maintain custody of an object. It is beneficial to use the limited tracking resources efficiently. To this end, an optimal scheduling algorithm is being developed based on maximizing Information Gain (IG) [1, 2]. An initial version, whereby the optimal schedule is determined for a single sensor in a passive optical tracking mode, is currently deployed at Mt Stromlo. The main objective of this development was to generate an interface at the tracking station to parse the tasking generated by the IG-scheduler and automatically collect observations. The tracking system automation software developed by EOS facilitates the experiments and the

interface was developed for the tracking system to accept the tasking. The feedback loop where the schedule is updated using the updated states and co-variances after the data collection is yet to be automated and is dependent on the automation of the orbit element generation. More sophisticated multi-sensor algorithms for maximizing information gain are in development and can be deployed comparatively easily once ready now that the interface is complete.

Manual catalogue maintenance is an expensive process which worsens as the catalogue grows in size. The cost of manual checking of data validity and generating orbital fits is prohibitive. For the SERC catalogue, the data post-processing and track correlation has been automated and can run using any state vector and covariance. The two state vector types that are used currently are internally generated orbital states and associated covariances, or a Two Line Element (TLE)[1] state and pseudo-covariance. The orbital element generation has been automated, fitting the observation data collected by the sensors. The procedure runs a Batch Least Squares process, where the dominant perturbation forces are fitted.

The Mt Stromlo station was tasked every night starting 22nd May 2016 using the IG-based scheduler for the target list which included the objects of interest presented in the next section.

3.1 Objects of interest from close approaches with Optus assets

The primary goal of the recent tracking campaign was to track objects identified in close approaches with Optus assets to assist with the building of the catalogue and conjunction assessment capabilities. The initial focus has been on the automation of the tracking data delivery and processing, orbit element generation, and subsequent cueing of the telescope. The new elements and predictions will then be used in the regular conjunction assessments that are currently running on the TLE catalogue. An example of the TLE-based analysis may be found in [3]. Tab. 1 shows the objects that were identified in close approach warnings with the Optus active fleet as of May 22nd 2017.

Tab. 1. Table for the objects of interest identified during conjunction assessments with Optus assets

International Designator	Name	NORAD ID	Period [mins]	Inc. [deg]	Apogee [km]	Perigee [km]	Size
1964-047A	SYNCOM 3	858	1437.41	2.24	35828	35796	LARGE
1974-017A	COSMOS 637	7229	1428.92	8.93	35829	35463	LARGE
1976-107A	EKRAN 1	9503	1435.36	11.52	36020	35524	LARGE
1974-017F	SL-12 R/B(2)	11567	1425.76	8.78	35796	35372	LARGE
1980-016A	RADUGA 6	11708	1436.97	13.09	35826	35782	LARGE
1982-103E	SL-12 R/B(2)	13630	1434.98	13.75	35800	35729	LARGE
1983-098A	GALAXY 2	14365	1436.78	14.99	35818	35782	MEDIUM
1985-055A	INTELSAT 511	15873	1438.34	15.19	35871	35790	LARGE
1986-044A	GORIZONT 12	16769	1435.06	14.59	35798	35735	LARGE
1976-092F	SL-12 R/B(2)	17872	1435.47	11.41	35825	35724	LARGE
1989-098A	RADUGA 24	20367	1435.13	15.24	35791	35745	LARGE
1990-094A	GORIZONT 21	20923	1434.4	14.99	35783	35724	LARGE
1992-088A	COSMOS 2224	22269	1435.67	14.3	35808	35749	LARGE
1997-016A	THAICOM 3	24768	1458.21	7.94	36586	35851	LARGE
1998-044B	CZ-3B R/B	25405	638.28	18.64	35754	603	LARGE
2002-002A	INSAT 3C	27298	1434.15	0.34	35754	35742	SMALL
1979-101G	SATCOM 3 DEB	29004	793.93	9.41	35901	8147	SMALL
2009-010B	SL-12 R/B(2)	34265	1439.68	4.89	35870	35843	LARGE
2009-018A	BEIDOU G2	34779	1434.55	4.62	36132	35381	LARGE
2012-069B	BLOCK DM-SL R/B	39021	648.94	0.23	35532	1370	LARGE
2014-010C	BREEZE-M R/B	39614	1589.75	1.58	41842	35644	LARGE

[1] https://www.space-track.org/, accessed 15-Sep-17.

For the objects contained in Tab. 1, the total number of tracks collected since the IG-based schedules were implemented at Mt Stromlo is shown in Fig. 2.

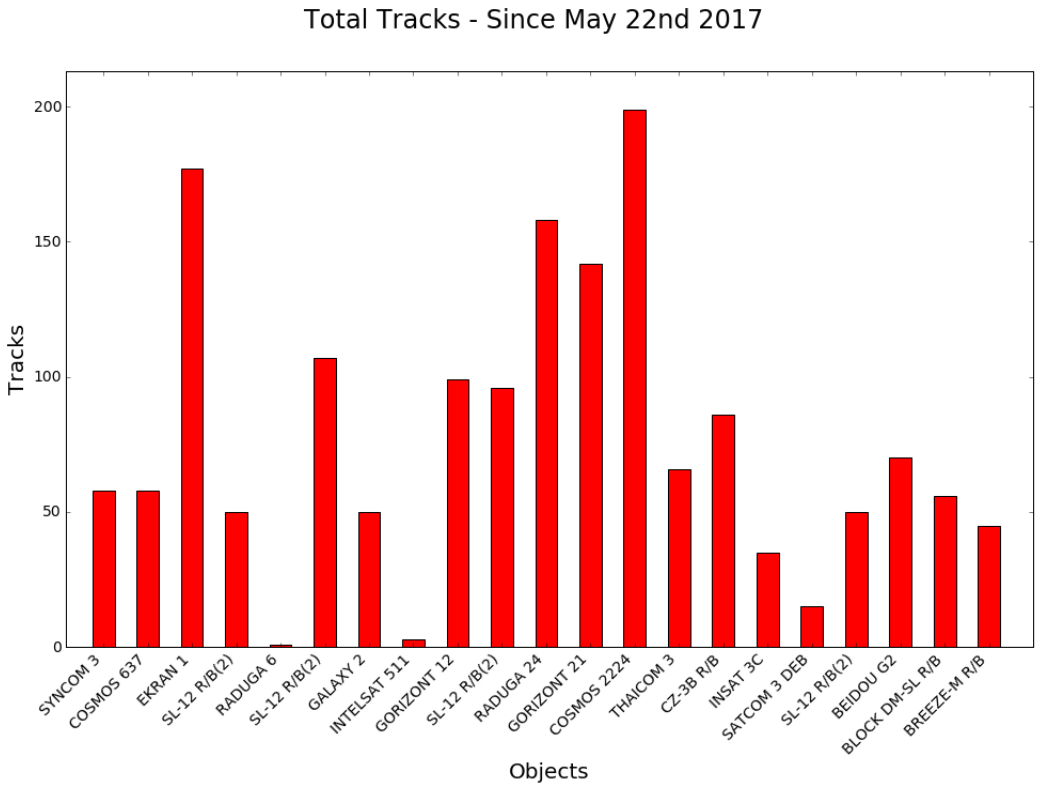

Fig. 2. Total number of tracks collected for the objects in Tab. 1 since the information gain based schedules have been implemented at Mt Stromlo.

4. DATA PROCESSING

4.1 Passive optical observation post-processing

The tracking system when operated in passive mode returns observations with the epoch, azimuth, and elevation. These are then passed to the post-processor which uses the previous state vector (TLE or SERC state vector) and propagates the state and covariance to the observation epoch where the observations are rejected or accepted based on a probability gate. All uncorrelated observations are removed during this process. The observations that are not rejected then pass through to astrometric calibration and axis rate generation where the azimuth and elevation rates of change are estimated using the fitting process described in [4]. The observation file outputs are delivered in three different files:

1. Uncalibrated full rate (not astrometrically corrected, i.e., mount model accuracy);
2. Calibrated full rate (astrometrically corrected);
3. Fitted, calibrated if exists, else uncalibrated.

If there is no state vector then the observations run through the process and the fitted points are generated for a later track association, for example, an admissible region track correlation. Uncorrelated observations can arise from misdetections during cloudy periods and are removed and put into an uncorrelated tracks directory.

4.1.1 Pointing accuracy

Part of the post-processing is to assess the accuracy of the pointing and is used as a metric to indicate whether the mount model needs to be corrected/calibrated. This is assessed using calibration objects such as geodetic satellites

tracked by the International Laser Ranging Service[2] and astrometric observations. An example of a mount accuracy assessment is contained in Fig. 3, where the truth pointing is derived from using Consolidated Prediction Format[3] (CPF) data as the reference orbit and calculating the corresponding slant range vector from Mt Stromlo.

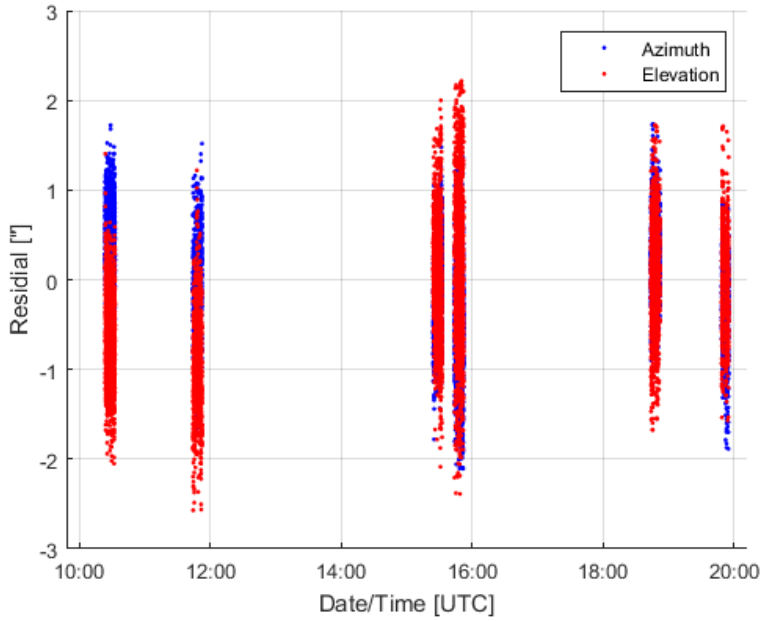

Fig. 3: Example of a calibrated mount accuracy assessment for the 30 June 2017. The plot shows azimuth and elevation residuals in arc seconds versus time in UTC. The truth pointing data is derived from accurate CPF reference orbits.

Regular accuracy assessments are needed to maintain a precise database of observations and subsequent orbital elements. Corrupting an orbit determination fitting process with uncorrelated tracks and/or erroneous measurements is likely to lead to divergence, or worse, convergence to a bad solution. For regular catalogue maintenance this is inconvenient. For conjunction assessments an incorrect orbit prediction can be catastrophic.

4.2 Passive optical observation and laser range post-processing

Optical and laser ranging data was collected in July 2017 at the new debris tracking facility at Learmonth, WA. During this data collection, Lageos 1 was tracked regularly and azimuth, elevation and range observations were collected. This section shows the results of the post-processing applied to the angles and range data. With the generation of the rates of change, the slant range vector and its rate of change can be used to provide state vector information using the following equation [5]:

$$\boldsymbol{r} = \boldsymbol{r}_{SITE} + \boldsymbol{\rho}$$

$$\boldsymbol{v} = \dot{\boldsymbol{\rho}}$$

where $\boldsymbol{r}$, $\boldsymbol{r}_{SITE}$, and $\boldsymbol{v}$ are the satellite position vector, the station position vector, and the satellite velocity vector in Earth-Centred Earth-Fixed (ECEF) coordinates, respectively. The vectors $\boldsymbol{\rho}$ and $\dot{\boldsymbol{\rho}}$ are the slant range vector and velocity in ECEF, respectively.

Several tracks of Lageos 1 were processed and the state vectors for each fitted observation were produced. The accuracy of the generated states was then assessed using the CPF reference orbits from the ILRS. Fig. 4 shows the results of the comparison.

[2] https://ilrs.cddis.eosdis.nasa.gov/ , accessed 13-Sep-17.
[3] https://ilrs.cddis.eosdis.nasa.gov/data_and_products/formats/cpf.html, accessed 15-Sep-17.

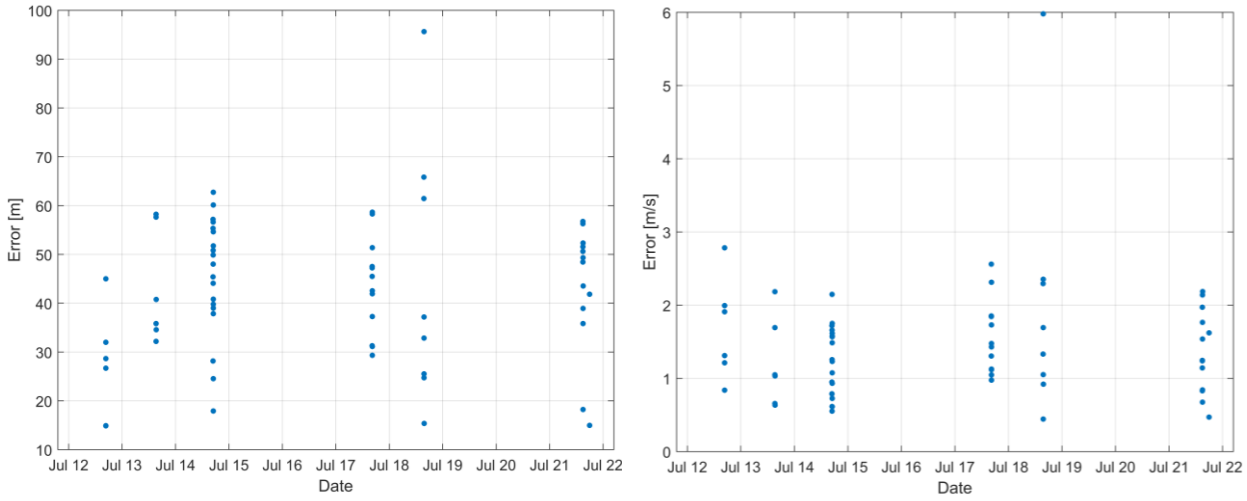

Fig. 4. Euclidean position and velocity errors of the ECEF states generated directly from the observations for Lageos 1 when compared to accurate CPFs.

The average position error over all of the states was found to be 42.6 metres, and the average velocity error was found to be 1.45 metres per second. This accuracy would not be achievable without a well calibrated and stable telescope mount and accurate range measurements.

These state vectors can be propagated individually or fitted in an orbit determination process. If propagated individually then the instantaneous observation error will directly affect the results whereas in a fitting process the effects of the outliers is reduced as long as there are not too many outliers. Fig. 5 shows the result of fitting an orbit to the observations whose residuals were reported in Fig. 4. The average position error over 7 days is 40.1 metres and the maximum is 67.5 metres.

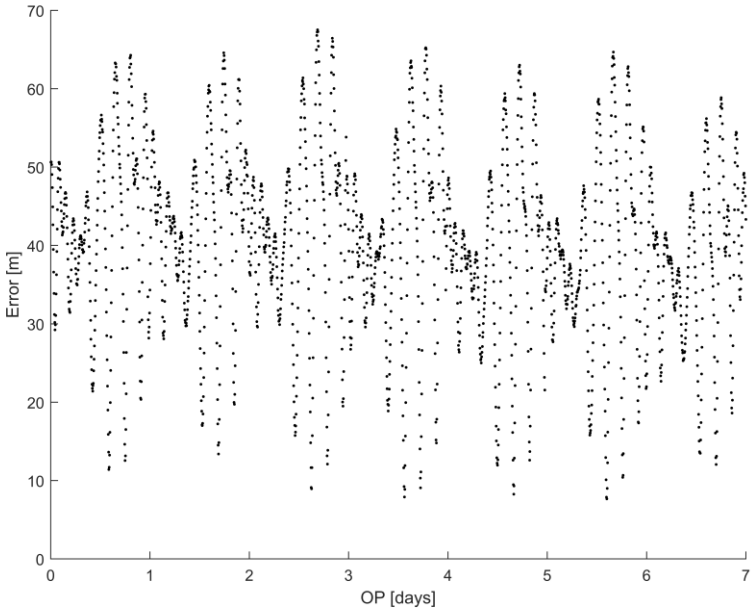

Fig. 5. Plot of the orbit prediction error resulting from fitting the ECEF position and velocity observations for Lageos 1. The residuals are calculated as the Euclidean position difference between the orbit prediction and the accurate ILRS CPFs.

5. ORBIT DETERMINATION RESULTS

As part of the automation of the orbit element generation, the newly generated elements are validated against prior observations not included in the fit span. This can give an indication of the propagation accuracy and the chance of reacquisition and is one of the validation techniques currently employed in the SERC catalogue maintenance. Provided here are results for three near-GEO objects and a highly elliptically object which were of interest during conjunction assessments with Optus assets, see Tab. 1. The results of up to 28 separate orbit determination processes using corrected data collected on different dates at Mt Stromlo observatory are discussed, with spans ranging from 3 to 10 days. The back propagation span was 15 days.

Fig. 6, Fig. 7, and Fig. 8 show boxplots of the azimuth and elevation residuals as a function of the number of days the orbital predictor back propagated for Galaxy 2, Gorizont 21 and COSMOS 2224, respectively. The number of observation passes (not the number of observations as each pass contains many observations) for each propagation day are indicated above the upper whiskers of the boxplots.

In Fig. 6, the interquartile range of the residuals are within 10 arcsec for up to 5 days with sub-arcsecond medians; moving beyond 5 days the accuracy is more variable. It is evident that either a lower quality prediction and/or poorer measurements are causing spreads of up to approximately 15–20 arcsec in the interquartile range in some cases. Nevertheless, the median azimuth and elevation residuals are within 5 arcsec after two weeks in all but two cases.

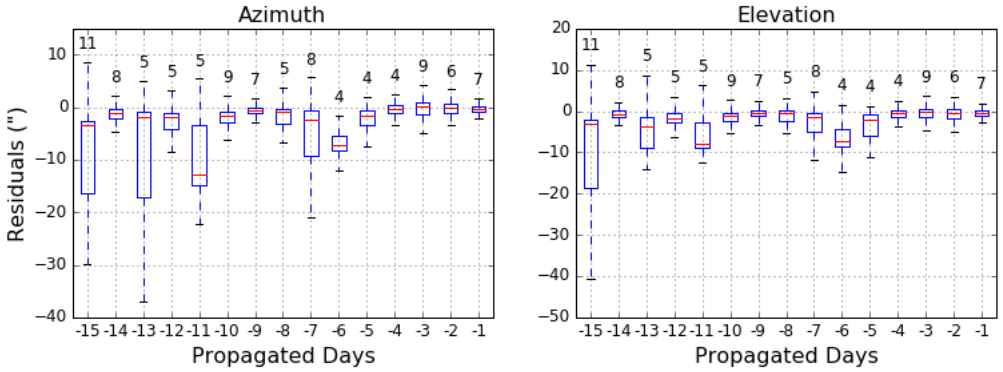

Fig. 6. Back propagated state vector compared with previous observations not contained in the orbit determination window for Galaxy 2 (NORAD ID 14365). 13 separate orbit determinations are summarized with fit spans ranging from 3 to 10 days.

In Fig. 7 the results are better for Gorizont 21 than the Galaxy 2 case and there were more orbital elements available for testing. Fig. 8 shows the orbit propagation results for Cosmos 2224. The results of the orbit propagations are good and the residuals are small over a 15 day span.

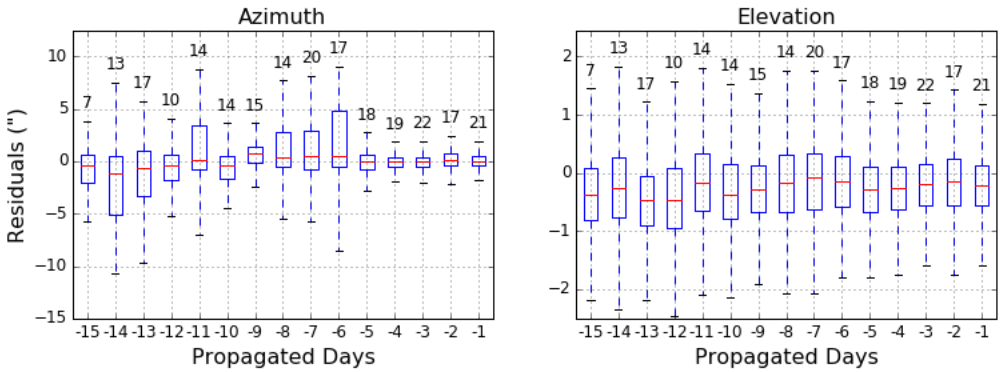

Fig. 7. Back propagated state vector compared with previous observations not contained in the orbit determination window for Gorizont 21 (NORAD ID 20923). 28 separate orbit determinations are summarized with fit spans ranging from 3 to 10 days.

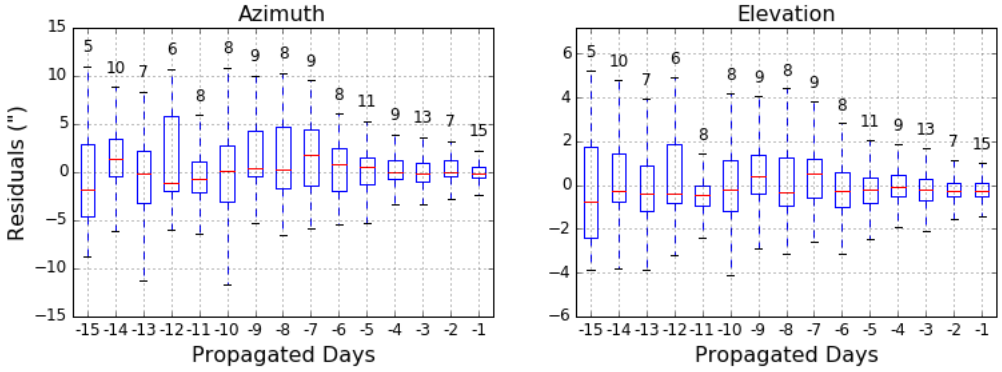

Fig. 8. Back propagated state vector compared with previous observations not contained in the orbit determination window for Cosmos 2224 (NORAD ID 22269). 24 separate orbit determinations are summarized with fit spans ranging from 3 to 10 days.

Fig. 6, Fig. 7, and Fig. 8 indicate that the many of these cases would fall within a few arc-seconds of the telescope boresight on a reacquisition attempt. These objects are in near-circular orbits and are relatively easy to acquire in a narrow field of view. In the next case an object with a highly elliptical orbit is considered. BLOCK DM-SL R/B has a perigee of 1,370 km and an apogee of 35,532 km and due to the elliptical nature of the orbit, the azimuth and elevation residuals are not a suitable metric to indicate the orbital error and as such, in Fig. 9, the orbital arc length Δr is presented as a function of the number of back propagated days.

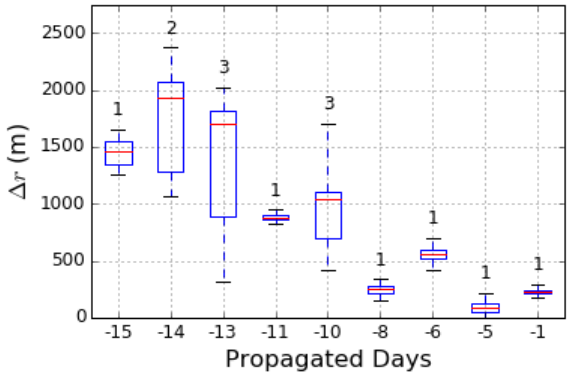

Fig. 9. Back propagated state vector compared with previous observations not contained in the orbit determination window for BLOCK DM-SL R/B (NORAD ID: 39021). 5 separate orbit determinations are summarized with fit spans ranging from 3 to 10 days.

Fig. 9 shows that the orbital arc-length of the object has a maximum value of under 2.5 km after two weeks. In this case there were only a few orbital elements available for propagation, however, the accuracy of these results are encouraging for catalogue maintenance and conjunction assessments for objects in elliptical orbits.

6. DISCUSSION

This accuracy of the orbital elements being generated for the SOC was presented. Large improvements in the accuracy of the measurements has been achieved by implementing metrics and tests to assess the telescope mount accuracy. The post-processing algorithms have improved the orbit element generation process by minimizing the corruption from erroneous observation data and manual intervention in the automated process has reduced. There are still cases that require manual intervention but the number has reduced significantly. Rules for different orbit regimes are being developed, particularly for the objects in highly elliptical orbits.

The post-processing of data from active laser ranging allows for accurate orbital state vectors to be constructed directly from the observations. An orbit determination process can then fit the data and solve for other parameters such as the ballistic coefficient. The examples presented here were for Lageos 1 which in a cooperative, spherical object. Future studies will consider the utility of the method for unknown debris in elliptical orbits.

The buildup of the SERC catalogue is continuing and improving in accuracy as refined processing methods are implemented. Once an interface is built to allow users not on the local network to receive the orbital elements, multiple areas of research currently being pursued will benefit such as the parallel conjunction assessments, nonlinear and non-Gaussian error propagation, optimized scheduling, and improved station cueing and post-processing. Then the orbit determination process will be improved by relaxing the assumption of spherically symmetric bodies and including recent advancements in the characterization of debris objects using light curves.

The number of objects involved in close approaches with Optus satellites has increased since the 22nd of May date. These will be included in a later analysis when full automation of the conjunction assessment process has been achieved. The research programs in the SAM group at SERC are being integrated together and will form a Conjunction and Threat Warning Service. The implementation of research outcomes into an operational system can be involved. The loop will be closed on the IG-scheduling so that the orbital states and covariances that are determined during the automated orbit determination are included in the next catalogue schedule update.

7. ACKNOWLEDGEMENTS

The authors would like to acknowledge the support of the Cooperative Research Centre for Space Environment Management (SERC Limited) through the Australian Government's Cooperative Research Centre Programme.

8. REFERENCES

1. Gehly, S. and J. Bennett, *Incorporating Target Priorities in the Sensor Tasking Reward Function*, in *Advanced Maui Optical and Space Surveillance Technologies Conference*. 2015: Maui, Hawaii.
2. Gehly, S., B. Jones, and P. Axelrad, *Sensor Allocation for Tracking Geosynchronous Space Objects.* Journal of Guidance, Control, and Dynamics, 2016: p. 0-0.
3. Flegel, S., et al., *An analysis of the 2016 Hitomi breakup event.* Earth, Planets and Space, 2017. **69**(1): p. 51.
4. Bennett, J.C. and S. Gehly, *Extracting more information from passive optical tracking observations for reliable orbit element generation*, in *Advanced Maui Optical and Space Surveillance Technologies Conference*. 2016: Maui, Hawaii.
5. Vallado, D.A., *Fundamentals of Astrodynamics and Applications*. Third ed. 2007: Microcosm Press, Hawthorne, CA and Springer, New York, NY.